Tumor Radiosensitization by Antiinflammatory Drugs: Evidence for a New Mechanism Involving the Oxygen Effect

Nathalie Crokart,[1,2] Kim Radermacher,[1,2] Bénédicte F. Jordan,[1,2] Christine Baudelet,[1,2] Gregory O. Cron,[1] Vincent Grégoire,[3] Nelson Beghein,[1,2] Caroline Bouzin,[4] Olivier Feron,[4] and Bernard Gallez[1,2]

[1]Laboratory of Medicinal Chemistry and Radiopharmacy, [2]Laboratory of Biomedical Magnetic Resonance, [3]Laboratory of Pharmacology and Therapeutics, [4]Laboratory of Molecular Imaging and Experimental Radiotherapy, Université Catholique de Louvain, Brussels, Belgium

Abstract

We hypothesized that nonsteroidal antiinflammatory drugs (NSAIDs) might enhance tumor radiosensitivity by increasing tumor oxygenation (pO_2), via either a decrease in the recruitment of macrophages or from inhibition of mitochondrial respiration. The effect of four NSAIDs (diclofenac, indomethacin, piroxicam, and NS-398) on pO_2 was studied in murine TLT liver tumors and FSaII fibrosarcomas. At the time of maximum pO_2 (t_{max}, 30 minutes after administration), perfusion, oxygen consumption, and radiation sensitivity were studied. Local pO_2 measurements were done using electron paramagnetic resonance. Tumor perfusion and permeability measurements were assessed by dynamic contrast-enhanced magnetic resonance imaging. The oxygen consumption rate of tumor cells after *in vivo* NSAID administration was measured using high-frequency electron paramagnetic resonance. Tumor-infiltrating macrophage localization was done with immunohistochemistry using CD11b antibody. All the NSAIDs tested caused a rapid increase in pO_2. At t_{max}, tumor perfusion decreased, indicating that the increase in pO_2 was not caused by an increase in oxygen supply. Also at t_{max}, global oxygen consumption decreased but the amount of tumor-infiltrating macrophages remained unchanged. Our study strongly indicates that the oxygen effect caused by NSAIDs is primarily mediated by an effect on mitochondrial respiration. When irradiation (18 Gy) was applied at t_{max}, the tumor radiosensitivity was enhanced (regrowth delay increased by a factor of 1.7). These results show the potential utility of an acute administration of NSAIDs for radiosensitizing tumors, and shed new light on the mechanisms of NSAID radiosensitization. These results also provide a new rationale for the treatment schedule when combining NSAIDs and radiotherapy. (Cancer Res 2005; 65(17): 7911-6)

Introduction

Cyclooxygenase-2 (COX-2) and its derivative prostanoids play an important role in the pathogenesis and evolution of a variety of cancers. A large number of neoplasms (primary and metastatic) overexpress COX-2, a condition often associated with more advanced or aggressive cancer and adverse prognosis. The tumor-promoting activities of COX-2 and its prostaglandins are mediated via several mechanisms, including conversion of procarcinogens to carcinogens, stimulation of tumor cell growth, prevention of apoptotic cell death, promotion of angiogenesis and immunosuppression (1–10). Several reviews have summarized evidence that nonsteroidal antiinflammatory drugs (NSAID) and, in particular, selective COX-2 inhibitors, are potentially interesting in cancer therapy (2–6, 11). However, the enthusiasm was recently hampered by evidence of cardiovascular side effects (increase in the incidence of myocardial infarction) when using COX-2 inhibitors during long-term treatments (12). Thus, a reconsideration of the risk benefit profile when using COX-2 inhibitors, as well as the optimal schedule to improve anticancer treatments, is likely necessary.

In chronic treatments, the desired therapeutic effects of COX-2 inhibitors are primarily immunostimulation and the inhibition of angiogenesis (10, 13–15). Interestingly, however, an acute and direct acute radiosensitization effect has also been shown for several COX-2 inhibitors. Proposed mechanisms for this effect have included an enhancement of radioinduced apoptosis, an effect on the cell cycle (G_2M arrest) and an inhibition of the repair from sublethal radiation damage (10, 15, 16). Thus far, there has been no study using NSAIDs which has investigated a possible radiosensitization effect mediated by oxygen, the most powerful radiosensitizing agent.

We hypothesized that NSAIDs could be important modulators of tumor oxygenation. The rationale for this hypothesis is based on a possible dual effect of NSAIDs on the oxygen consumption in tumors. First, NSAIDs are known to uncouple mitochondrial oxidative phosphorylation with important consequences on cell oxygen consumption (17–20). Second, antiinflammatory drugs could affect the recruitment and migration of macrophages. For example, it was recently shown that NS-398, a selective COX-2 inhibitor, increases macrophage migration inhibitory factor expression in prostate cancer cells (21). Because macrophages are cells that consume oxygen at a high rate (22), an inhibition of their recruitment could lead to an increase in tumor oxygenation.

Using two different tumor models, we show that the administration of NSAIDs has a profound effect on tumor oxygenation. In order to identify the factors responsible for this reoxygenation of the tumors, we characterized changes in the tumor microenvironment: perfusion, permeability, interstitial fluid pressure (IFP), oxygen consumption, and presence of macrophages. We also investigated the sensitivity of tumors to irradiation at the time of maximal reoxygenation.

Materials and Methods

Animal Tumor Models

Two different syngeneic tumor models were implanted in the gastrocnemius muscle in the rear leg of male mice (20-25 g, B&K, Hull,

Requests for reprints: Bernard Gallez, Laboratory of Biomedical Magnetic Resonance, Université Catholique de Louvain, CMFA/REMA Avenue Mounier 73.40, B-1200 Brussels, Belgium. Phone: 32-2764-2792; Fax: 32-2764-2790; E-mail: Gallez@cmfa.ucl.ac.be.

doi:10.1158/0008-5472.CAN-05-1288

United Kingdom): the transplantable liver tumor TLT in NMRI mice and the FSaII tumor in C3H mice. All treatments were applied when the tumor reached 8.0 ± 0.5 mm. All experiments were conducted according to national animal care regulations.

Treatments

Anesthesia. Animals were anesthetized by inhalation of isoflurane mixed with 21% oxygen in a continuous flow (1.5 L/h), delivered by a nose cone. Induction of anesthesia was done using 3% isoflurane. It was then stabilized at 1.2% for a minimum of 15 minutes before any measurement. The temperature of the animals was kept constant using IR light, a homeothermic blanket control unit, or a flow of temperature-controlled warm air.

Antiinflammatory drugs. All antiinflammatory drugs were administrated by i.p. injection. Diclofenac was administrated at a dose of 20 mg/kg (Voltaren, Novartis, Brussels, Belgium, diluted in saline to a final concentration of 5 mg/mL); Piroxicam at 25 mg/kg (Feldene, Pfizer, Brussels, Belgium, diluted in saline to 10 mg/mL); Indomethacin at 2 mg/kg (Indocid, Merck Sharp and Dohme, Brussels, Belgium, diluted in saline to 0.6 mg/mL); and NS-398 [*N*-[2(cyclohexyloxy) 4-nitrophenyl-methanesulfonamide] at 10 mg/kg (Alexis Biochemicals, Zandhoven, Belgium, diluted in DMSO to 2 mg/mL).

Oxygen Measurements

Electron paramagnetic resonance (EPR) oximetry (using charcoal as the oxygen-sensitive probe) was used to evaluate tumor oxygenation changes using a protocol previously described (23, 24). EPR spectra were recorded using an 1.2 GHz EPR spectrometer (Magnettech, Berlin, Germany). Mice were injected 2 days before EPR in the center of the tumor using the suspension of charcoal (100 mg/mL, 50 μL injected, particle size <25 μm). These localized EPR measurements record the average pO_2 in a volume of about 10 mm^3 (24).

Perfusion Measurements

Magnetic resonance imaging measurements. Perfusion measurements were done via dynamic contrast-enhanced magnetic resonance imaging (DCE-MRI; ref. 25). MRI was done at 4.7 T with a 40 cm inner diameter bore system (Bruker Biospec, Ettlingen, Germany). T1-weighted gradient-recalled echo images were obtained with repetition time = 40 ms, echo time = 4.9 ms, 1.6 mm slice thickness, flip angle = 90 degrees, matrix = 64 × 64, FOV = 4 cm, 25 kHz receiver bandwidth, 2.56 seconds per scan. The contrast agent was a rapid-clearance blood pool agent, P792 (Vistarem, Laboratoire Guerbet, Aulnay sous Bois, France). P792 (MW, 6.47 kDa) is a monogadolinium macrocyclic compound based on a gadolinium tetraazacyclododecanetetraacetic acid structure substituted by hydrophilic (dextran) arms. Its R1 relaxivity in 37°C human serum albumin, 4% at 4.7 T is 9 $mM^{-1}s^{-1}$ P792 was injected at a dose of 0.042 mmol Gd/kg (26). We used the following protocol: after 12 baseline images had been acquired, P792 was given i.v. within 2 seconds (50 μL/40 g mouse) and the enhancement kinetics were continuously monitored for 8 minutes (200 total scans). This allowed sufficient sampling of the signal intensity-time curve to track the fast increase in tissue enhancement for viable tumor following bolus arrival. After 8.5 minutes of rapid imaging, a slower data set was acquired to monitor the washout of the contrast agent. For this second set, 60 scans were acquired at a temporal resolution of 60 seconds (1 hour total).

Kinetic analysis. An operator-defined region of interest encompassing the tumor was analyzed on a voxel-by-voxel basis to obtain parametric maps. Using cluster analysis, voxels for which typical signal enhancement curves were observed were then selected for pharmacokinetic analysis (27). Contrast agent concentration as a function of time after P792 injection ($C(t)$) was estimated by comparing the tumor signal intensity as a function of time ($S(t)$) with the signal intensity in a reference tissue (muscle) with known T1 (28). The tracer concentration changes were fitted to a two-compartment pharmacokinetic model as previously described (25, 28, 29). Parametric images for ν_p (the blood plasma volume per unit volume of tissue), K^{Trans}_{in} (the influx volume transfer constant into extravascular extracellular space from plasma), and k_{ep} (the fractional rate of efflux from the interstitial space back to the blood) were computed, with only the statistically significant parameter estimates being displayed.

Interstitial Fluid Pressure Measurements

The IFP was measured using a "wick-in-needle" apparatus (30, 31). An 18-gauge needle with a 1 mm side hole located about 5 mm from the needle tip was connected to a Stryker pressure monitor system (Stryker, 295-1 Pressure), specially designed for measuring tissue fluid pressures. The entire system was filled with saline water. The calibration of the pressure was checked before each experiment. A zero reference was obtained by placing the needle to one side at tumor height and resetting the system. The needle was inserted approximately into the center of the tumor, then 50 μL of saline was injected to measure IFP.

Oxygen Consumption Rate Evaluation

An EPR method was used which has been described previously (32). Briefly, the spectra were recorded on a Bruker EMX EPR spectrometer operating at 9 GHz. Mice were sacrificed and the tumors were excised, trypsinized for 30 minutes, and cell viability determined with Trypan blue exclusion. Cells (2×10^7/mL) were suspended in 10% dextran in complete medium. A neutral nitroxide, ^{15}N 4-oxo-2,2,6,6-tetramethylpiperidine-d_{16}-15 N-1-oxyl at 0.2 mmol/L (CDN Isotopes, Pointe-Claire, Quebec, Canada), was added to 100 μL aliquots of tumor cells that were then drawn into glass capillary tubes. The probe (0.2 mmol/L in 20% dextran in complete medium) was calibrated at various O_2 levels between 100% nitrogen and air so that the line width measurements could be related to O_2 at any value. Nitrogen and air were mixed in an Aaborg gas mixer, and the oxygen content was analyzed using a Servomex oxygen analyzer OA540. The sealed tubes were placed into quartz EPR tubes and the samples were maintained at 37°C. Because the resulting line width reports on pO_2, it was possible to calculate oxygen consumption rates by measuring the pO_2 in the closed tube as a function of time and subsequently computing the slope of the resulting plot.

Immunohistochemistry

Dissected tumors embedded in Tissue-Tek optimum cutting temperature compound were frozen in liquid nitrogen–cooled isopentane. Cryosections (5 μm) were fixed in acetone. Endogenous peroxidase activity was inhibited by peroxidase blocking reagent (DakoCytomation, Heverlee, Belgium). Slides were incubated with rat monoclonal anti-CD11b antibody (PharMingen, Erembodegem, Belgium), followed by rabbit anti-rat immunoglobin (DakoCytomation). Both antibodies were diluted in PBS/1% bovine serum albumin. Envision system (DakoCytomation) was used for detection. The peroxidase was detected using 3-amino-9-ethylcarbazole (AEC, DakoCytomation).

Tumor Regrowth Delay Assay

The FSaII tumor (8.0 ± 0.5 mm) was locally irradiated with a 250 kV X-ray irradiator (RT 250, Philips Medical System, 1.2 Gy/min). The tumor was centered in a 3 cm diameter circular irradiation field. After treatment, tumor diameter was measured every day using a digital caliper until the diameter reached 16 mm, at which time the mice were sacrificed. A linear fit was done for diameters ranging from 8 to 16 mm, allowing determination of the time to reach a particular size for each mouse.

Experimental Design

Oximetry. Three basal pO_2 values were measured every 10 minutes before the treatment. After injection, the pO_2 values were acquired every 5 minutes for a total time of 1 hour. The measurements were done for six groups of TLT tumors: two control groups [injected with saline (n = 4) or with DMSO (n = 4)] and four groups treated with Diclofenac (n = 5), Indomethacin (n = 6), Piroxicam (n = 4), or NS-398 (n = 7). Two groups of FSaII tumors were injected with NS-398 (n = 7) or with DMSO (n = 4). Further experiments were done exclusively with NS-398 on the FSaII tumor model.

Dynamic contrast-enhanced magnetic resonance imaging. Two groups of FSaII tumors were used: one control group (DMSO, n = 5) and one group treated with NS-398 30 minutes before the dynamic MR sequence (n = 5).

Interstitial fluid pressure. Two groups of FSaII tumors were used: one control group (DMSO, n = 4) and one group treated with NS-398 30 minutes before the measurement (n = 4).

Oxygen consumption. These experiments were carried out on two groups of FSaII tumors. The consumption rate was determined for the same number of cells 30 minutes after treatment with DMSO (control, n = 4) or NS-398 (n = 4).

Tumor regrowth delay. Four groups of FSaII tumors were used for this study. The first group (n = 8) was a control injected with NS-398 on day 0, without irradiation. The second group (n = 7) was irradiated at a dose of 18 Gy 30 minutes after injection of DMSO. The third group (n = 6) was irradiated at a dose of 18 Gy 30 minutes after injection of NS-398. Finally, the fourth group (n = 6) was irradiated at a dose of 18 Gy 20 minutes after breathing carbogen (95% O_2 and 5% CO_2).

Immunohistochemistry. Two groups of FSaII tumors were used in this study. For both groups, the mice were sacrificed for tumor excision 30 minutes after administration of DMSO (n = 6) or NS-398 (n = 6).

Statistical Analysis

Means ± SEs were compared using the unpaired Student's t test. For regrowth delay, a one-way ANOVA Tukey's multiple comparison test was used.

Results

Effect of nonsteroidal antiinflammatory drugs on tumor oxygenation. Several NSAIDs belonging to different chemical classes (piroxicam, indomethacin, diclofenac, and NS-398) were tested for their possible effect on tumor oxygenation. After administration of all these compounds, we observed a rapid increase in pO_2 in TLT tumors (Figs. 1 and 2). The maximal pO_2 was reached ~30 minutes after treatment, with the tumor pO_2 remaining elevated until at least 1 hour after administration. For further investigation of tumor model dependency, the selective COX-2 inhibitor NS-398 was chosen to be tested in FSaII tumors as well. Using this compound, we observed a rapid increase in the oxygenation for both tumor models (Fig. 2). At maximal reoxygenation time, the increase in pO_2 was 4.2 ± 0.4 mm Hg for the FSaII model and 6.0 ± 1.1 mm Hg for the TLT model.

Effect of NS-398 on hemodynamic parameters (perfusion, permeability, and interstitial fluid pressure). The blood perfusion and vascular permeability of tumor was investigated using DCE-MRI 30 minutes after drug administration (Fig. 3). A significant decrease of 50.5 ± 12.3% (P < 0.01, unpaired t test) in the percentage of perfused pixels (pixels showing non-zero values of K_{trans} or k_{ep}) was observed 30 minutes after injection, showing that perfusion is significantly reduced by NS-398. The value of the plasmatic volume fraction (v_p) was unchanged, whereas the permeability (K_{trans} and k_{ep}) was significantly decreased. Figure 3 shows histogram data and cumulative histogram data summed for all animals in each group. NS-398-treated tumors show a more homogeneous, narrow histogram for k_{ep} and K_{trans} than the control group. The extracellular and extravascular volume (v_e) tended to increase, although not significantly (39.8 ± 16.7%, P = 0.093). To corroborate this increase in v_e, a measurement of the IFP was done 30 minutes after NS-398 administration. The IFP was significantly increased (Fig. 4): 15.7 ± 0.4 mm Hg for the control group versus 19.5 ± 0.9 mm Hg for the treated group (P < 0.05, unpaired t test).

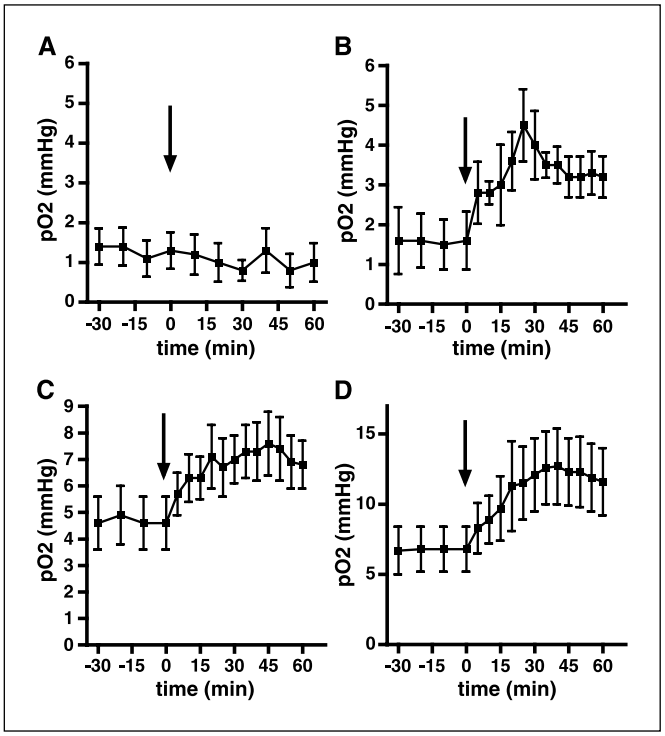

Figure 1. Tumor pO_2 measured by EPR oximetry in TLT tumors as a function of time. *Arrows,* injection time of the drug. *A,* saline (n = 4); *B,* piroxicam (n = 4); *C,* diclofenac (n = 5); *D,* indomethacin (n = 6).

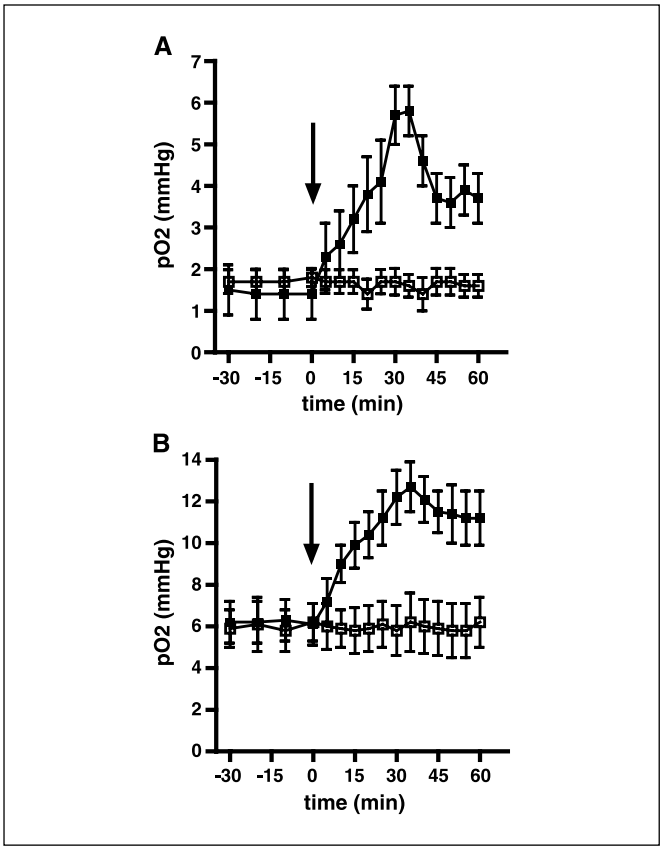

Figure 2. Tumor pO_2 measured by EPR oximetry as a function of time in FsaII tumors (*A*); DMSO (n = 4; □); NS-398 (n = 7; ■); and TLT tumors (*B*). DMSO (n = 4; □); NS-398 (n = 7; ■). *Arrows,* the injection times of the drug.

Effect of NS-398 on oxygen consumption. Because the increase in pO_2 was not related to an increase in perfusion, the tumor oxygen consumption was investigated 30 minutes after treatment. The administration of NS-398 significantly decreased the rate of oxygen consumption (Fig. 5): 0.31 ± 0.02 μmol/L/min for the control (DMSO) group versus 0.19 ± 0.01 μmol/L/min for the treated group (P < 0.01, unpaired t test).

Effect of NS-398 on tumor-infiltrating macrophages. Immunohistochemistry with CD11b antibody was done on tumors to investigate whether the decrease in oxygen consumption may be caused by a decrease in the number of infiltrating macrophages.

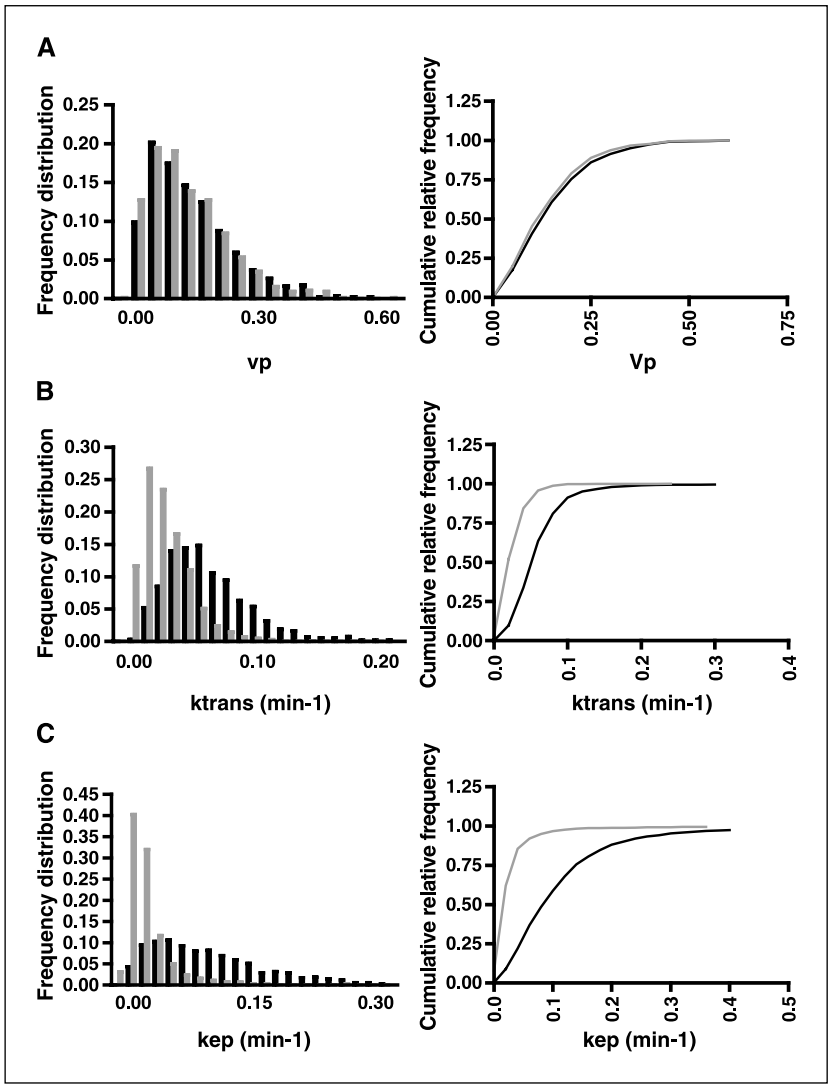

Figure 3. Hemodynamic parameters measured in FsaII tumors using DCE-MRI. *A,* plasma volume fraction (v_p); *B,* influx volume transfer constant from plasma into the interstitial space (K_{trans}); *C,* the fractional rate of efflux from the interstitial space back to the plasma (k_{ep}). The results are presented in frequency distribution (left) and cumulative relative frequency (right). Data for control mice injected with DMSO (n = 5; in black). Data for the NS-398 treated mice (n = 5; in gray) 30 minutes after administration of the drug. Note that v_p was unchanged whereas K_{trans} and k_{ep} were significantly decreased after NS-398 administration.

The number of macrophages in the center of the tumor was low. Most macrophages were located in the periphery of the tumor and near the connection with the muscle (host tissue). No difference was observed between tumors excised from mice treated with NS-398 or treated with DMSO alone (data not shown).

Improvement of radiation efficacy. To determine whether NS-398 had an effect on the tumor response to radiotherapy, FSaII tumor-bearing mice were treated with irradiation alone, with a combination of NS-398 and irradiation, or with a combination of carbogen and irradiation. The results of the regrowth delay assay are shown in Table 1. All irradiated groups showed a significant regrowth delay in comparison with the control group (non irradiated). When combining irradiation with the administration of NS-398 at the time of maximal reoxygenation, the regrowth delay was significantly increased compared with irradiation alone (4.8 $\pm$ 0.3 days versus 2.8 $\pm$ 0.2 days, P < 0.001 one-way ANOVA). Using NS-398, the regrowth delay is therefore increased by a factor of 1.7. We also observed that the efficacy of NS-398 is comparable to the respiration of carbogen (regrowth delay 4.7 $\pm$ 0.3 days), because there was no significant difference in these regrowth delays (P > 0.05 one-way ANOVA).

Discussion

Oxygen effect and parameters responsible for this effect. For the first time, we report that the administration of NSAIDs (nonselective and selective inhibitors of COX-2) induce a dramatic increase in tumor oxygenation (Figs. 1 and 2). This phenomenon was rapid, occurring within the first 30 minutes

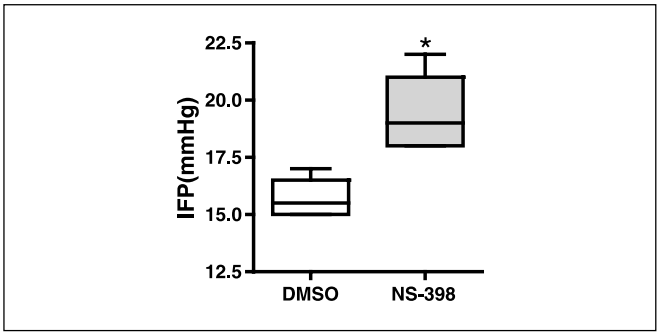

Figure 4. Measurement of IFP after administration of DMSO alone or NS-398 30 minutes after administration (FsaII tumors). □, DMSO (n = 4); ■, NS-398 (n = 4).

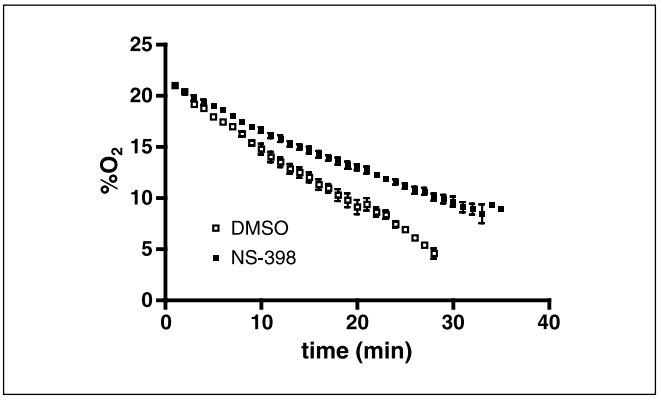

Figure 5. Effect of NS-398 administration on the tumor oxygen consumption rate in FsaII tumors. *In vivo* NS-398-pretreated cells consumed oxygen significantly more slowly than cells treated with DMSO alone. □, DMSO (n = 4); ■, NS-398 (n = 4).

after administration. Having identified the temporal kinetics of this increase in oxygenation, we then used multiple modalities to investigate the possible mechanisms responsible for this effect. Generally speaking, tumor reoxygenation may result from an increase in oxygen delivery and/or a decrease in oxygen consumption. The results obtained from DCE-MRI (Fig. 3) preclude the possibility that the increase in tumor oxygenation is due to an increase in perfusion. The plasma volume fraction was unchanged, and the number of voxels in tumors that receive the contrast agent was decreased after administration of antiinflammatory agents. We also found that the permeability was decreased and the extravascular extracellular space was increased. This latter increase was correlated with an increase in IFP as measured by the wick-in-needle technique (Fig. 4). The decrease in permeability after administration of NSAIDs is not surprising, because it is well-established that a major effect of inflammation is to increase permeability (33).

Because the increase in tumor oxygenation was not due to an increase in perfusion, we can assume that the reoxygenation of the tumor is linked to an effect on oxygen consumption. It has been predicted theoretically that modification of oxygen consumption is much more efficient at affecting the tumor oxygenation than modification of oxygen delivery (34). This was confirmed by measuring the oxygen consumption rate by tumor cells (Fig. 5): we found that oxygen consumption was significantly reduced after administration of NS-398. Two different mechanisms could potentially be responsible for the decrease in oxygen consumption: a direct effect on the mitochondrial respiration (well established in the literature; refs. 17–20) or an effect on the recruitment of macrophages (21). An effect on the recruitment of macrophages is unlikely to be the factor responsible for the decrease in oxygen consumption. The immunohistochemistry study revealed no difference in the number and repartition of macrophages between treated and control tumors. The results of our study strongly support the first hypothesis, according to which the effect of NSAIDs on tumor oxygenation is related to the well-established uncoupling of oxidative phosphorylation in mitochondria, with a consequent decrease in oxygen consumption.

A new approach for combining nonsteroidal antiinflammatory drugs and radiotherapy: timing and safety considerations. The magnitude of the increase in tumor oxygenation observed in this study is, in principle, sufficient to enhance the response of tumors to radiation therapy. We previously found in the same tumor model that drugs which are able to increase the pO_2 to the same level were responsible for a radiosensitization effect (35–37). Here, we showed a dramatic increase in the tumor response when the irradiation was applied at the time of maximal reoxygenation induced by the NSAIDs. This effect is remarkable, considering that it is comparable to the radiosensitization effect observed with carbogen breathing.

The oxygen effect observed with the NSAIDs should be considered an additional effect to previously described mechanisms, i.e., enhancement of radioinduced apoptosis, effect on the cell cycle (G_2M arrest) and inhibition of the repair from sublethal radiation damage (10, 15, 16). All of these mechanisms suggest that NSAIDs should be given before irradiation to obtain the radiosensitization effect. Moreover, the demonstration of the oxygen effect gives unique insight into the timing to achieve maximal sensitization. The finding that NSAIDs are very efficient when given acutely is particularly interesting, given the current debate on the usefulness of chronic administration of selective inhibitors of COX-2 due to their cardiovascular toxicity (12). Moreover, our results show that the oxygen effect is also present when using NSAIDs that do not belong to the class of COX-2 inhibitors for which no long-term cardiovascular toxicity has been shown.

Table 1. Regrowth delays of four groups of FSaII tumors

Group	Time to reach 12 mm (days)	Regrowth delay (days)
Control	2.9 ± 0.2	
DMSO + 18 Gy	5.7 ± 0.1***	2.8 ± 0.2
NS-398 + 18 Gy	7.7 ± 0.2***	4.8 ± 0.3
Carbogen + 18 Gy	7.6 ± 0.3***	4.7 ± 0.3

NOTE: The control group only injected once with NS-39 8 (n = 8). Second group treated with DMSO 30 minutes before 18 Gy irradiation (n = 7). Third group treated with NS-398 30 minutes before 18 Gy irradiation (n = 6). Fourth group treated with carbogen 20 minutes before 18Gy irradiation (n = 6). Results are mean ± SE. Statistical analysis: one-way ANOVA Tukey's multiple comparison test.
***, $P < 0.001$.

Conclusion

For the first time, we show that NSAIDs increase tumor oxygenation shortly (30 minutes) after administration. The mechanisms responsible for this oxygen effect involve a decrease in oxygen consumption. This oxygen effect may play an important role in the radiosensitizing properties of these drugs. Our findings provide unique insights into the administration schedule of these drugs as adjuvants to anticancer therapies.

Acknowledgments

Received 4/13/2005; revised 6/6/2005; accepted 6/17/2005.

Grant support: Belgian National Fund for Scientific Research (FNRS), the Télévie, the Fonds Joseph Maisin, and the "Actions de Recherches Concertées-Communauté Française de Belgique-ARC 04/09-317." Christine Baudelet and Benedicte Jordan are Research Fellows of the FNRS. Olivier Feron is a Research associate of the FNRS.

The costs of publication of this article were defrayed in part by the payment of page charges. This article must therefore be hereby marked *advertisement* in accordance with 18 U.S.C. Section 1734 solely to indicate this fact.

The authors thank Guerbet Laboratories (Roissy, France) for providing P792.

References

1. Milas L, Mason K, Liao Z, et al. Role of cyclooxygenase-2 (COX-2) and its inhibition in tumor biology and radiotherapy. In: Nieder C, Milas L, Ang KK, editors. Modification of radiation response. Germany: Springer-Verlag; 2003. p. 241–58.
2. Choy H, Milas L. Enhancing radiotherapy with cyclooxygenase-2 enzyme inhibitors: a rational advance? J Natl Cancer Inst 2003;95:1440–52.
3. Gasparini G, Longo R, Sarmiento R, Morabito A. Inhibitors of cyclo-oxygenase 2: a new class of anticancer agents? Lancet Oncol 2003;4:605–15.
4. Subongkot S, Frame D, Leslie W, Drajer D. Selective cyclooxygenase-2 inhibition: a target in cancer prevention and treatment. Pharmacotherapy 2003;23:9–28.
5. Zha S, Yegnasubramanian V, Nelson WG, Isaacs WB, De Marzo AM. Cyclooxygenases in cancer: progress and perspective. Cancer Lett 2004;215:1–20.
6. Subbaramaiah K, Dannenberg AJ. Cyclooxygenase 2: a molecular target for cancer prevention and treatment. Trends Pharmacol Sci 2003;24:96–102.
7. Warner TD, Mitchell JA. Cyclooxygenases: new forms, new inhibitors, and lessons from the clinic. FASEB J 2004;18:790–804.
8. Blanke C. Role of COX-2 inhibitors in cancer therapy. Cancer Invest 2004;22:271–82.
9. Haller DG. COX-2 inhibitors in oncology. Semin Oncol 2003;30:2–8.
10. Nakata E, Mason KA, Hunter N, et al. Potentiation of tumor response to radiation or chemoradiation by selective cyclooxygenase-2 enzyme inhibitors. Int J Radiat Oncol Biol Phys 2004;58:369–75.
11. Thun MJ, Henley SJ, Patrono C. Nonsteroidal anti-inflammatory drugs as anticancer agents: mechanistic, pharmacologic, and clinical issues. J Natl Cancer Inst 2002;94:252–66.
12. Couzin J. Drug safety. FDA panel urges caution on many anti-inflammatory drugs. Science 2005;307:1183–5.
13. Pyo H, Choy H, Amorino GP, et al. A selective cyclooxygenase-2 inhibitor, NS-398, enhances the effect of radiation *in vitro* and *in vivo* preferentially on the cells that express cyclooxygenase-2. Clin Cancer Res 2001;7: 2998–3005.
14. Petersen C, Petersen S, Milas L, Lang FF, Tofilon PJ. Enhancement of intrinsic tumor cell radiosensitivity induced by a selective cyclooxygenase-2 inhibitor. Clin Cancer Res 2000;6:2513–20.
15. Raju U, Nakata E, Yang P, Newman RA, Ang KK, Milas L. *In vitro* enhancement of tumor cell radiosensitivity by a selective inhibitor of cyclooxygenase-2 enzyme: mechanistic considerations. Int J Radiat Oncol Biol Phys 2002;54:886–94.
16. Komaki R, Liao Z, Milas L. Improvement strategies for molecular targeting: Cyclooxygenase-2 inhibitors as radiosensitizers for non-small cell lung cancer. Semin Oncol 2004;31:47–53.
17. Mahmud T, Rafi SS, Scott DL, Wrigglesworth JM, Bjarnason I. Nonsteroidal antiinflammatory drugs and uncoupling of mitochondrial oxidative phosphorylation. Arthritis Rheum 1996;39:1998–2003.
18. Moreno-Sanchez R, Bravo C, Vasquez C, Ayala G, Silveira LH, Martinez-Lavin M. Inhibition and uncoupling of oxidative phosphorylation by nonsteroidal anti-inflammatory drugs: study in mitochondria, submitochondrial particles, cells, and whole heart. Biochem Pharmacol 1999;57:743–52.
19. Somasundaram S, Rafi S, Hayllar J, et al. Mitochondrial damage: a possible mechanism of the "topical" phase of NSAID induced injury to the rat intestine. Gut 1997;41:344–53.
20. Jacob M, Bjarnason I, Rafi S, Wrigglesworth J, Simpson RJ. A study of the effects of indometacin on liver mitochondria from rats, mice and humans. Aliment Pharmacol Ther 2001;15:1837–42.
21. Meyer-Siegler K. COX-2 specific inhibitor, NS-398, increases macrophage migration inhibitory factor expression and induces neuroendocrine differentiation in C4-2b prostate cancer cells. Mol Med 2001;7:850–60.
22. James PE, Jackson SK, Grinberg OY, Swartz HM. The effects of endotoxin on oxygen consumption of various cell types *in vitro*: an EPR oximetry study. Free Radic Biol Med 1995;18:641–7.
23. Gallez B, Baudelet C, Jordan BF. Assessment of tumor oxygenation by electron paramagnetic resonance: principles and applications. NMR Biomed 2004; 17:240–62.
24. Gallez B, Jordan B, Baudelet C, Misson PD. Pharmacological modifications of the partial pressure of oxygen in tumors. Evaluation using *in vivo* EPR oximetry. Magn Reson Med 1999;42:627–30.
25. Baudelet C, Ansiaux R, Jordan BF, Havaux X, Macq B, Gallez B. Physiological noise in murine solid tumor using T2*-weighted gradient-echo imaging: a marker of tumour acute hypoxia? Phys Med Biol 2004;49:3389–411.
26. Fan X, Medved M, River JN, et al. New model for analysis of dynamic contrast enhanced MRI data distinguishes metastatic from nonmetastatic transplanted rodent prostate tumors. Magn Reson Med 2004;51:487–94.
27. Baudelet C, Gallez B. Cluster analysis of BOLD fMRI time series in tumors to study the heterogeneity of hemodynamic response to treatment. Magn Reson Med 2003;49:985–90.
28. Tofts PS. Modeling tracer kinetics in dynamic Gd-DTPA MR imaging. J Magn Reson Imaging 1997;7:91–101.
29. Tofts PS, Brix G, Buckley DL, et al. Estimating kinetic parameters from dynamic contrast-enhanced T(1)-weighted MRI of a diffusable tracer: standardized quantities and symbols. J Magn Reson Imaging 1999; 10:223–32.
30. Fadnes HO, Reed RK, Aukland K. Interstitial fluid pressure in rats measured with a modified wick technique. Microvasc Res 1977;14:27–36.
31. Boucher Y, Kirkwood JM, Opacic D, Desantis M, Jain RK. Interstitial hypertension in superficial metastatic melanomas in humans. Cancer Res 1991;51:6691–4.
32. Jordan BF, Beghein N, Aubry M, Gregoire V, Gallez B. Potentiation of radiation-induced regrowth delay by isosorbide dinitrate in FSAII murine tumors. Int J Cancer 2003;103:138–41.
33. el-Ghazaly M, Kenawy S, Khayyal MT, et al. Effect of exposure to radiation on the inflammatory process and its influence by diclofenac. Br J Pharmacol 1985;85:45–50.
34. Secomb TW, Hsu R, Ong ET, Gross JF, Dewhirst MW. Analysis of the effects of oxygen supply and demand on hypoxic fraction in tumors. Acta Oncol 1995;34:313–6.
35. Jordan BF, Misson PD, Demeure R, Baudelet C, Beghein N, Gallez B. Changes in tumor oxygenation/perfusion induced by the NO donor, isosorbide dinitrate, in comparison with carbogen: monitoring by EPR and MRI. Int J Radiat Oncol Biol Phys 2000;48:565–70.
36. Jordan BF, Gregoire V, Demeure RJ, et al. Insulin increases the sensitivity of tumors to irradiation: involvement of an increase in tumor oxygenation mediated by a nitric oxide-dependent decrease of the tumor cells oxygen consumption. Cancer Res 2002;62: 3555–61.
37. Ansiaux R, Baudelet C, Jordan BF, et al. Thalidomide radiosensitizes tumors through early changes in the tumor microenvironment. Clin Cancer Res 2005;11: 743–50.